Journal of Alzheimer's Disease 79 (2021) 127–139
DOI 10.3233/JAD-200578
IOS Press

The Differential Influence of Immune, Endocytotic, and Lipid Metabolism Genes on Amyloid Deposition and Neurodegeneration in Subjects at Risk of Alzheimer's Disease

Grazia Daniela Femminella[a], Denise Harold[b], James Scott[a], Julie Williams[c] and Paul Edison[a,*] for the Alzheimer's Disease Neuroimaging Initiative[1]
[a]*Imperial College London, London, United Kingdom*
[b]*Dublin City University, Dublin, Ireland*
[c]*School of Medicine, Cardiff University, Cardiff, United Kingdom*

Accepted 12 October 2020

Abstract.
Background: Over 20 single-nucleotide polymorphisms (SNPs) are associated with increased risk of Alzheimer's disease (AD). We categorized these loci into immunity, lipid metabolism, and endocytosis pathways, and associated the polygenic risk scores (PRS) calculated, with AD biomarkers in mild cognitive impairment (MCI) subjects.
Objective: The aim of this study was to identify associations between pathway-specific PRS and AD biomarkers in patients with MCI and healthy controls.
Methods: AD biomarkers ([^{18}F]Florbetapir-PET SUVR, FDG-PET SUVR, hippocampal volume, CSF tau and amyloid-β levels) and neurocognitive tests scores were obtained in 258 healthy controls and 451 MCI subjects from the ADNI dataset at baseline and at 24-month follow up. Pathway-related (immunity, lipid metabolism, and endocytosis) and total polygenic risk scores were calculated from 20 SNPs. Multiple linear regression analysis was used to test predictive value of the polygenic risk scores over longitudinal biomarker and cognitive changes.
Results: Higher immune risk score was associated with worse cognitive measures and reduced glucose metabolism. Higher lipid risk score was associated with increased amyloid deposition and cortical hypometabolism. Total, immune, and lipid scores were associated with significant changes in cognitive measures, amyloid deposition, and brain metabolism.
Conclusion: Polygenic risk scores highlights the influence of specific genes on amyloid-dependent and independent pathways; and these pathways could be differentially influenced by lipid and immune scores respectively.

Keywords: Alzheimer's disease, biomarkers, genetic risk, polygenic score, SNPs

[1]Data used in preparation of this article were obtained from the Alzheimer's Disease Neuroimaging Initiative (ADNI) database (https://adni.loni.usc.edu). As such, the investigators within the ADNI contributed to the design and implementation of ADNI and/or provided data but did not participate in analysis or writing of this report. A complete listing of ADNI investigators can be found at: https://adni.loni.usc.edu/wp-content/uploads/how_to_apply/ADNI_Acknowledgement_List.pdf.

*Correspondence to: Dr. Paul Edison, MBBS, MRCP, MPhil, PhD, FRCP, FRCPI, Senior Clinical Lecturer, Imperial College London and Visiting Professor, Cardiff University, Neurology Imaging Unit, Imperial College London, 1st Floor, B Block, Hammersmith Hospital Campus, Du Cane Road, London. W12 0NN, UK. Tel.: +442083833725; Fax: +442033134320; E-mail: paul.edison@imperial.ac.uk.

INTRODUCTION

Alzheimer's disease (AD) is the most common cause of dementia affecting individuals over 65 years of age [1]; 50 million people have dementia worldwide, and there are nearly 10 million new cases every year [2]. With the aging population, the burden of AD on healthcare systems and society is set to rise [3, 4]. The failure of clinical trials to improve cognitive function and halt disease progression in AD, together with the demonstration of a long preclinical phase of the disease, highlights the need for early intervention, and indeed challenges our understanding of the disease.

Subjects with mild cognitive impairment (MCI) are at increased risk of developing AD dementia with 50% of amyloid positive MCI subjects converting to AD within 2 years [5, 6]. Thus, predicting which MCI patients will actually progress is of utmost importance, which is now helped by biomarkers including cerebrospinal fluid (CSF) levels of amyloid-β (Aβ) and tau, and neuroimaging modalities [7, 8].

Individual risk for AD is determined by genetic, environmental, and demographic factors, as well as interactions among them [9]. Unlike familial AD, where genetic mutations in *APP*, *PSEN1*, and *PSEN2* are mostly fully penetrant and of autosomal dominant inheritance, sporadic AD (sAD) also has significant heritability [10]. Inheritance of the ε4 allele of the apolipoprotein E (*APOE*) is the most important genetic risk factor for sAD, increasing risk 3-fold in heterozygotes and 15-fold in homozygotes [11].

Recently, genome wide association studies (GWAS) have been able to identify over 30 risk loci associated with the development of sAD [12–18]. Although the effect of the single locus might be small, a polygenic risk score (PRS) allows us to evaluate the combined effects of gene variants. To date, several studies have used this polygenic approach to estimate the risk of AD progression and to evaluate the association of AD genetic risk with endophenotypes of the disease. Harrison et al. have demonstrated the association between a total PRS and hippocampal thinning in healthy individuals [19]. Other studies have shown that an association exists between PRS and CSF biomarkers and disease progression [20], as well as between PRS and plasma inflammatory biomarkers [21]. A PRS can improve the diagnostic accuracy of *APOE* alone at identifying AD cases [22], predict the age of AD onset [23], and can generally improve risk prediction in healthy older adults [24, 25]. Moreover, a PRS has been demonstrated to predict cognitive decline and neurodegeneration in subjects at risk of AD [26]. Recently, pathway-specific PRS have been associated with AD biomarkers, grouping risk loci together according to their biological functions [27] and, in some cases, finding that pathway-specific PRS might hold higher predictive value over total PRS [28].

In this study we categorized 20 of the single nucleotide polymorphisms (SNPs) susceptibility loci into the three pathways of endocytosis, immunity, and lipid metabolism to create a PRS for each of them, and also a total PRS. We selected SNPs identified by the International Genomics of Alzheimer's Project (IGAP) [12, 14]. The immune pathway contained nine loci (*CR1, INPP5D, MEF2C, HLA-DRB5/HLA-DRB1, EPHA1, CLU, MS4A6A, ABCA7, CD33*), the endocytosis pathway contained six loci (*BIN1, CD2AP, EPHA1, PICALM, SORL1, CD33*), and the lipid pathway contained three (*CLU, SORL1, ABCA7*), with five loci overall contributing to more than one pathway. The total PRS comprised all the above plus seven variants that, due to lack of strong biological evidence, were not attributed to any of the specific pathways (*NME8, ZCWPW1, PTK2B, CELF1, FERMT2, SLC24A4/RIN3, CASS4*). These were compared against the main pathological substrates of AD: amyloid deposition (CSF Aβ and amyloid PET), tau aggregation (CSF phosphorylated tau), and neurodegeneration (CSF total tau, fludeoxyglucose (FDG) PET and MRI volumes). The aim was to identify possible associations between pathway-specific PRS and AD biomarkers in patients with MCI and healthy controls. To date, no previous study has compared PRS to such an extensive range of biomarkers [20, 24, 29].

METHODS

Data collection was downloaded from the Alzheimer's Disease Neuroimaging initiative (ADNI) from October 2017 to December 2017. ADNI is an ongoing international longitudinal study aimed at the identification of markers for the early detection and monitoring of AD such as proteomics, CSF tau and amyloid, MRI, FDG and tau PET scans, including baseline demographics of healthy controls (HC), MCI, and AD subjects. According to the ADNI guidelines, MCI is defined by a Mini-Mental State Examination (MMSE) score of 24–30, an education adjusted cut-off on the Logical Memory II subscale from the Wechsler Memory Scale

clinical dementia rating scale (CDR) of 0.5, and preserved daily functioning at home confirmed by a study partner. For this study, we included FDG-PET and amyloid ([^{18}F]Florbetapir) PET standard uptake value ratio (SUVR), hippocampal volumes, CSF total and phosphorylated tau, CSF Aβ, neurocognitive tests (ADAS COG-11 and 13, CDR-SB, MMSE), *APOE4* status, and level of education, which were obtained from the ADNI dataset. We retrieved baseline and 24-months follow up data for 258 HC and 451 MCI subjects.

For Florbetapir scans, 370 MBq (10.0 mCi) ± 10% of tracer was injected, and scans were acquired in 4 × 5 min frames with acquisition time of 50–70 min post-injection. For, FDG PET, 185 MBq (5.0 mCi) ± 10% of tracer was injected and scans were acquired for 30 min (6 × 5 min frames) with an acquisition time of 30–60 min post-injection. For image processing, either six 5-min frames (ADNI1) or four 5-min frames (ADNI GO/2) are acquired 30 to 60 min post-injection. Each extracted frame is co-registered to the first extracted frame of the raw image file (frame acquired at 30–35 min post-injection). Co-registered image is generated simply by averaging different time frames.

FDG-PET scans were analyzed using target to pons ratio as detailed in the ADNI protocol which provided SUVR for a set of pre-defined regions of interest (MetaROIs) based on coordinates cited frequently in other FDG studies comparing AD, MCI, and normal subjects and including left and right temporal lobe, left and right angular gyrus and the posterior cingulate. SUVR for FDG uptake were calculated using a pons/vermis reference region [30]. [^{18}F]Florbetapir-PET scans provided SUVR values for the frontal, parietal and temporal lobe, cingulate gyrus, the medial temporal lobe (MTL), for both the left and right side and the total cortical amyloid load, using the cerebellum as a reference region [31]. All regional values were derived from ADNI dataset. Data for hippocampal volume were derived from 3D-MPRAGE MRI scans using a semi-automated hippocampal volumetry tool.

Available genotype data for the ADNI cohort (818 individuals genotyped on the Illumina Omni2.5 array) was downloaded from the ADNI website and subjected to quality control. Individuals were excluded if they had a call rate <98%, were outliers on principal components analysis based on a pairwise identity by descent matrix, or were related to another genotyped ADNI participant at the level of first cousin or closer. Variants were excluded if they departed from Hardy-Weinberg equilibrium ($p < 10^{-4}$). As not all susceptibility SNPs identified through GWAS had been genotyped on the Illumina Omni2.5 array, IMPUTE2 was used to impute genotypes for these variants, using 1,000 Genomes haplotypes as a reference panel (Phase I integrated variant set release (produced using SHAPEIT2) in NCBI build 37 coordinates). All missing variants were successfully imputed with info scores >0.95. Imputed dosage data was converted to hard-called genotypes using GTOOL.

Immune, endocytotic, and lipid genome-wide significant PRS (GWS-PRS) were calculated in PLINK, based on 20 of the SNPs common variants identified by the meta-analysis conducted by the IGAP [12, 14] (see Supplementary Table 1 for the SNPs assigned to each pathway-specific score). Moreover, a total GWS-PRS was calculated. Weighted risk scores were calculated per person as the sum of the product of the number of risk alleles of the selected SNPs and the natural log of the corresponding odds ratio reported in the IGAP meta-analysis [12, 14]. To compare subjects with high or low GWS-PRS, the 10th and 90th percentile of each of the scores were calculated, with an approach also used by others [26].

Statistical analysis was performed using SPSS 25. Normality was evaluated with Kolmogorov-Smirnov test on the whole population. The total, immune, and endocytotic GWS-PRS were normally distributed, while the lipid GWS-PRS did not follow a normal distribution. Independent sample t test was used to compare normally distributed variables at baseline and paired sample t tests to determine significant difference at follow up. When the sample variable was non-linear, non-parametric Mann-Whitney U test was used. Simple linear regression was performed for normally distributed variables and Spearman's rank test was used to test correlation between the lipid GWS-PRS and biomarkers. Multiple linear regression analysis was conducted on the delta variables of biomarkers and cognitive measures testing the different GWS-PRS as predictors, with or without *APOE4* status, and adjusting for age and gender.

RESULTS

The baseline characteristics of the HC and MCI groups are shown in Table 1. As expected, the MCI group was significantly impaired in the neuropsychometric tests evaluated, compared to the HC. The number of *APOE4* carriers was similar between HC and MCI. Interestingly, the mean total and immune

Table 1
Baseline characteristics of healthy controls and MCI subjects

	HC		MCI	
		N		N
Male n (%)	131 (50.78)	258	271 (60.09)	451
Age mean (SD) (years)	74.71 (5.49)	258	72.52 (7.41)*	451
GWS SNP score mean (SD)	1.23 (0.16)	258	1.25 (0.16)*	451
Immune SNP score mean (SD)	0.42 (0.11)	258	0.44 (0.11)*	451
Endocytotic SNP score mean (SD)	0.55 (0.11)	258	0.56 (0.10)	451
Lipid metabolism SNP score mean (SD)	0.36 (0.07)	258	0.37 (0.08)	451
CDR-SB mean (SD)	0.03 (0.14)	258	1.43 (0.86)*	451
ADAS11 mean (SD)	5.85 (2.90)	258	9.57 (4.31)*	450
ADAS13 mean (SD)	9.16 (4.21)	258	15.34 (6.62)*	448
MMSE mean (SD)	29.07 (1.16)	258	27.92 (1.67)*	451
ApoE4 Non carrier n (%)	175 (67.8)	258	259 (57.4)	451
ApoeE4 Heterozygous n (%)	72 (27.9)	258	158 (35.0)	451
ApoeE4 Homozygous n (%)	11 (4.3)	258	34 (7.5)	451
Years of Education mean (SD)	16.43 (2.64)	258	16.01 (2.9)	451
Hx of Smoking n (%)	104 (40.30)	258	182 (40.4)*	451
Right handed n (%)	240 (93.0)	258	408 (90.5)	451

*Significant difference between HC and MCI at $p < 0.05$ Data displayed in the table is represented as mean (standard deviation), or number (percentage). N, number of total available subjects for which data was available; HC, healthy controls; MCI, mild cognitive impairment.

Table 2
Baseline biomarkers of healthy controls and MCI subjects

	HC		MCI	
		N		N
[^{18}F]Florbetapir Frontal lobe mean (SD)	1.30 (0.28)	141	1.39 (0.30)*	301
[^{18}F]Florbetapir Parietal lobe mean (SD)	1.32 (0.28)	141	1.40 (0.30)*	301
[^{18}F]Florbetapir Temporal lobe mean (SD)	1.23 (0.25)	141	1.30 (0.27)*	301
[^{18}F]Florbetapir Cingulate gyrus mean (SD)	1.42 (0.29)	141	1.50 (0.31)*	301
[^{18}F]Florbetapir Left MTL mean (SD)	1.22 (0.27)	141	1.31 (0.28)*	301
[^{18}F]Florbetapir Right MTL mean (SD)	1.26 (0.25)	141	1.33 (0.29)*	301
CSF Aβ mean (SD)	211.61 (59.68)	16	178.07 (55.80)	27
CSF tau mean (SD)	78.3 (51.66)	16	93.47 (40.34)	27
CSF p-tau mean (SD)	33.95 (18.85)	16	45.87 (27.68)	27
L Hippocampal volume mean (SD) (mm^3)	2315.20 (291.02)	19	1901.01 (361.07)*	19
R Hippocampal volume mean (SD) (mm^3)	2253.31 (358.51)	19	1909.00 (440.25)*	19
FDG Left angular gyrus mean (SD)	1.32 (0.12)	190	1.26 (0.16)*	373
FDG Right angular gyrus mean (SD)	1.31 (0.13)	190	1.26 (0.15)*	373
FDG Posterior cingulate gyrus mean (SD)	1.39 (0.14)	190	1.36 (0.17)*	373
FDG Left Temporal lobe mean (SD)	1.27 (0.13)	190	1.21 (0.14)*	373
FDG Right Temporal lobe mean (SD)	1.24 (0.12)	190	1.20 (0.12)*	373

*Significant difference between HC and MCI at $p < 0.05$ Data displayed in the table is represented as mean (standard deviation), or number (percentage). N, number of total available subjects for which data was available; HC, healthy controls; MCI, mild cognitive impairment.

GWS-PRS were higher in MCI compared to HC, while the endocytotic and lipid metabolism PRS were similar between the two groups. There was no difference between males and females in terms of any of the GWS-PRSs scores, both in the group as a whole and in HC and MCI separately.

When looking at the baseline biomarkers (Table 2), the MCI showed significantly higher brain Aβ deposition compared to HC, as detected by [^{18}F] Florbetapir-PET in all the predefined regions. Based on the cut-off of 1.1 for [^{18}F]Florbetapir in composite cortical region [31], 48/139 HC and 159/297 MCI were Aβ positive. The CSF levels of Aβ, tau, and *p*-tau were not significantly different between the two groups, although the CSF data were only available for a small subgroup of subjects (16 HC and 27 MCI). The biomarkers of neurodegeneration (hippocampal volume and FDG uptake in all the predefined regions) were significantly lower in MCI subjects compared to HC, as expected. When stratifying the population according to *APOE4* and Aβ status, we found that *APOE4* + /Aβ+ subjects ($n = 121$) had signifi-

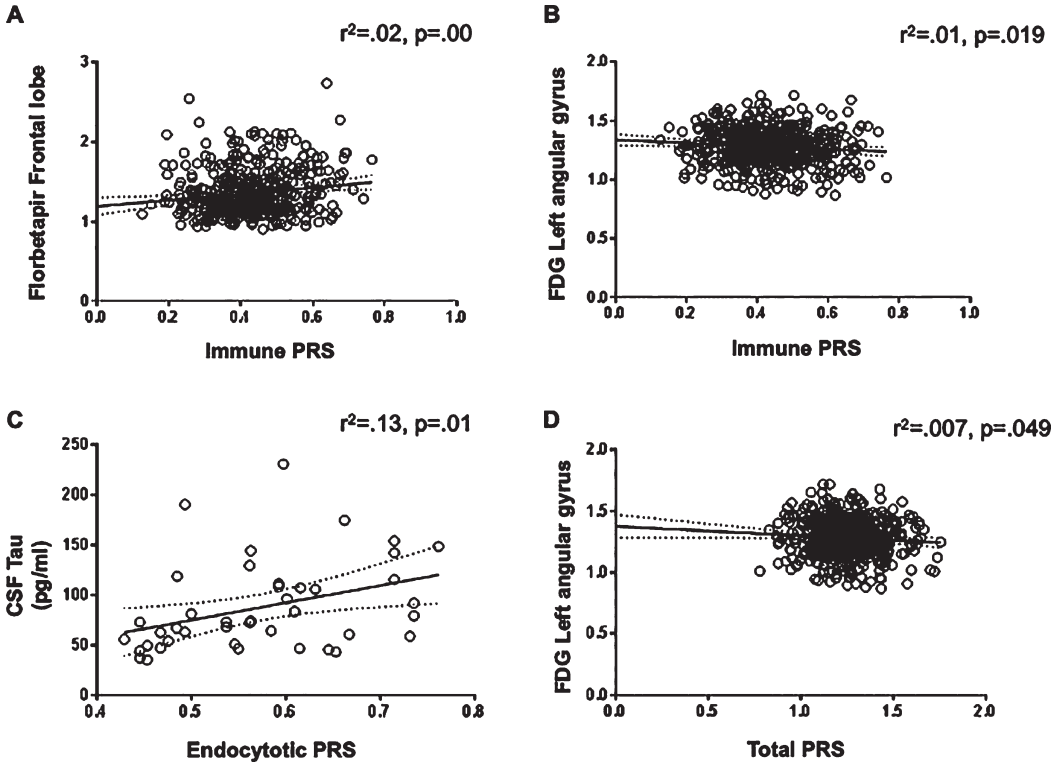

Fig. 1. Linear regression between genome-wide significant PRS and AD biomarkers. Direct association was shown between the immune PRS and [^{18}F]Florbetapir uptake in frontal lobe (A) while significant inverse association was shown between the immune PRS and FDG uptake in the left angular gyrus (B). The endocytotic PRS showed a significant direct association with CSF tau levels (C). The total PRS showed significant inverse association with FDG uptake in the left angular gyrus (D).

cantly higher GWS-PRSs compared to *APOE4*-/Aβ- ($n = 181$) subjects.

To evaluate the relationship between the GWS-PRSs and biomarkers at baseline, we run linear regression between the immnune, endocytotic, lipid, and total GWS-PRS and both CSF and imaging biomarkers. As shown in Fig. 1, significant inverse association was shown between the immune GWS-PRS and FDG uptake in the left angular gyrus ($r^2 = 0.01$, $p = 0.019$), while direct association were shown between the immune GWS-PRS and [^{18}F]Florbetapir uptake in frontal, temporal, parietal, mid-temporal lobes and cingulate gyrus (correlation with frontal [^{18}F]Florbetapir uptake is shown in Fig. 1, $r^2 = 0.02$, $p = 0.00$). The total GWS-PRS showed significant inverse association with FDG uptake in the left angular gyrus ($r^2 = 0.007$, $p = 0.049$). The endocytotic GWS-PRS showed a significant direct association with CSF tau levels ($r^2 = 0.13$, $p = 0.01$), while the lipid GWS-PRS did not show any significant correlations with any of the biomarkers.

To better clarify which biomarkers can be associated with the pathway-specific GWS-PRS, we compared the 10th and 90th percentile of each of the four GWS-PRS (total, immune, endocytotic, and lipid) to see how the low and high GWS-PRS groups differ in terms of biomarkers. The mean GWS-PRS values for 10th and 90th percentile and the number of subjects included in the percentile groups of each GWS-PRS are shown in Supplementary Table 2.

The 10th and 90th percentile groups of the total GWS-PRS differed significantly in terms of cognitive measures (CDR-SB, ADAS13, MMSE), [^{18}F]Florbetapir uptake and CSF tau levels (Supplementary Table 3). The comparison between 10th and 90th percentile of the immune GWS-PRS indicated that the two groups differed in terms of cognitive measures (CDR-SB, ADAS11, ADAS13) and FDG uptake in the left angular gyrus (Supplementary Table 4). There were no significant differences in any of the biomarkers when comparing the 10th and 90th percentiles of the endocytotic GWS-PRS. The 10th and 90th percentile groups of the lipid GWS-PRS dif-

fered significantly in terms of [^{18}F]Florbetapir uptake in all the predefined regions and FDG uptake in the left temporal lobe (Supplementary Table 5).

The 10th and 90th percentile groups of total, immune, and endocytotic GWS-PRS did not differ in terms of prevalence of *APOE4* carriers, while there were significantly more *APOE4* carriers in the 90th percentile of lipid GWS-PRS compared to the 10th percentile group (56.4% versus 43.6%, $p = 0.044$). Moreover, the 10th and 90th percentile groups of total, lipid, and endocytotic GWS-PRS did not differ in terms of prevalence of MCI subjects compared to control subjects. However, there were significantly more MCI subjects in the 90th percentile immune GWS-PRS group compared to the 10th percentile group (60.4% versus 39.6%, $p = 0.001$).

In the whole population, the parameters that significantly changed from baseline to follow up were: CDR-SB, ADAS11, ADAS13, MMSE, CSF Aβ, CSF total tau, FDG uptake in all the predefined regions, [^{18}F]Florbetapir uptake in all the predefined regions, left and right hippocampal volume (Supplementary Table 6).

We calculated delta variables for each of the above using the following formula: ((xf – xi)/xi)*100, where xf is the follow up value and xi is the baseline value.

Then we compared the delta variables between 10th and 90th percentile for each of the polygenic scores. The parameters showing significant differences are reported in Fig. 2.

Significant variations from baseline to follow up were observed in ADAS11 and ADAS13 scores, as well as in temporal FDG between 10th and 90th percentiles of total GWS-PRS.

A significant variation in MMSE scores and in frontal [^{18}F]Florbetapir uptake was observed between 10th and 90th percentiles of immune GWS-PRS, while 10th and 90th percentiles of lipid GWS-PRS showed significant longitudinal changes in MMSE scores and FDG uptake in the left angular gyrus.

Moreover, on a subset of 367 subjects, we retrieved information on stability or clinical progression at 24 months. Overall, 33 subjects progressed (from HC to MCI or from MCI to AD) and 334 remained stable. When looking at baseline GWS-PRSs scores in stable subjects versus progressing subjects, we did not find significant differences in the scores.

Finally, we performed multiple regression analysis for each of the delta variables, building two models including each of the GWS-PRSs as a predictor, with or without *APOE4* carrier status. Significant associations were observed only for changes in CDR-SB and FDG uptake in posterior cingulate and left temporal lobe, as shown in Table 3. Interestingly, the immune GWS-PRS was an independent predictor of FDG longitudinal change in posterior cingulate and left temporal lobe, even when *APOE* was not included in the model. The immune GWS-PRS was not significantly associated with changes in amyloid deposition, CSF biomarkers or cognitive measures. The total GWS-PRS was a significant predictor of CDR-SB changes, while the lipid score was not independently associated with any changes in the biomarkers. Overall, the variance explained by the models, with or without *APOE* status, was between 1.9% and 3.3%.

DISCUSSION

In this study we have demonstrated the association between GWS-PRS for critical molecular pathways involved in AD pathogenesis (immunity, endocytosis, and lipid metabolism) and biomarkers in a cohort of subjects at risk of AD. The calculation of the GWS-PRS has been performed based on the individual genetic risk from the 20 loci identified by IGAP. Our data indicate that higher immune GWS-PRS was associated with hypometabolism of the angular gyrus and worse cognitive performance at baseline and with increased longitudinal amyloid deposition. Moreover, immune GWS-PRS was an independent predictor of hypometabolism in the posterior cingulate and left temporal lobe. A higher lipid GWS-PRS was associated with increased cortical amyloid uptake and left temporal hypometabolism at baseline and with longitudinal reduction in FDG uptake. The endocytotic GWS-PRS correlated with baseline total CSF tau levels but not with longitudinal changes in any of the biomarkers, neither with baseline differences between high and low GWS-PRS. The total GWS-PRS, which includes all the 20 SNP scores, was associated with worse cognitive performance and higher total CSF tau levels at baseline, and with longitudinal changes in cognitive measures and temporal hypometabolism. Moreover, the total GWS-PRS was an independent predictor of CDR-SB longitudinal changes. To our knowledge, this is the first study aiming at evaluating all these biomarkers profiles changes in the AD risk trajectory and their association with gene variations grouped according to their function. The results of this study indicate which AD endophenotypes are more likely to be affected by genes involved in immunity, endocytosis, and lipid metabolism, shedding further light on the

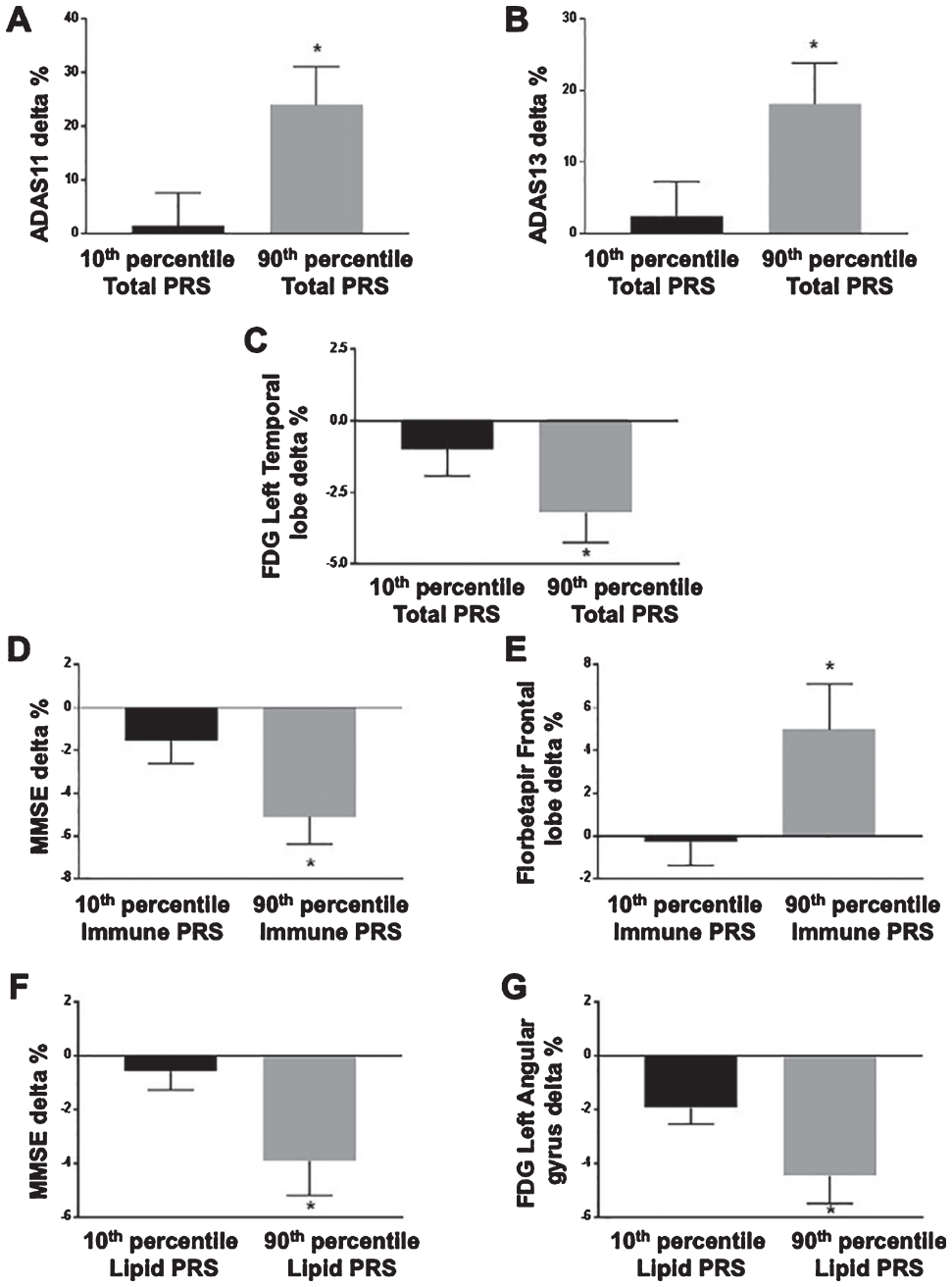

Fig. 2. Significant delta variables between 10th and 90th percentile of total, immune and lipid genome-wide significant PRS. Significant variations from baseline to follow up were observed in ADAS11 (A) and ADAS13 scores (B), as well as in temporal FDG (C) between 10th and 90th percentiles of total PRS. A significant variation in MMSE scores (D) and in frontal [^{18}F]Florbetapir uptake (E) was observed between 10th and 90th percentiles of immune PRS, while high and low lipid PRS showed significant longitudinal changes in MMSE scores (F) and FDG uptake in the left angular gyrus (G).

possible mechanisms underlying the 20 genes function. Indeed, as an endophenotype is influenced by fewer genetic risk factors than the disease as a whole, it can provide important information about the biological pathway through which a gene might act [32].

Other studies have evaluated PRS in AD progression, based on the hypothesis that an aggregated genetic risk score could perform better than any individual variant. Escott-Price et al. have recently demonstrated that PRS analysis has a good pre-

Table 3
Effects of genome-wide significant PRSs on longitudinal cognitive and biomarker changes

	Model A (without *APOE*)			Model B (with *APOE*)		
	β	95% CI	R2	β	95% CI	R2
	Regression coefficients for longitudinal CDR-SB variation					
Immune PRS	112.56	–30.17, 255.29		101.70	–40.90, 244.29	
Endocytotic PRS	78.28	–71.59, 228.15		62.59	–87.50, 212.68	
Lipid PRS	182.96	–18.36, 384.28		167.47*	–33.72, 368.65	0.024
Total PRS	**119.34***	19.48, 219.21	0.020	**106.30***	5.72, 206.89	0.028
	Regression coefficients for longitudinal variation in FDG uptake in posterior cingulate					
Immune PRS	**–5.26***	–10.31, –0.22	0.020	–4.78†	–9.81, 0.25	0.033
Endocytotic PRS	–1.19	–6.47, 4.09		–0.54	–5.81, 4.74	
Lipid PRS	–0.82	–7.94, 6.29		–0.12*	–7.21, 6.98	0.025
Total PRS	–3.28*	–6.73, 0.18	0.019	–2.76*	–6.23, 0.70	0.022
	Regression coefficients for longitudinal variation in FDG uptake in left temporal lobe					
Immune PRS	**–7.07***	–12.8, –1.34	0.020	**–6.76***	–12.50, –1.02	0.024
Endocytotic PRS	–2.35	–8.35, 3.66		–1.92	–7.95, 4.11	
Lipid PRS	–4.11	–12.20, 3.99		–3.65	–11.75, 4.46	
Total PRS	–4.06	–7.99, –0.13		–3.74	–7.70, 0.22	

All models are additionally adjusted for age and gender. *$p < 0.05$ and †$p < 0.01$ for the model. Significant PRS predictors within the model are in bold.

dictive value for AD in pathologically confirmed case-control series [33] and PRS have been validated in both Black and White populations [34]. PRS analysis has also suggested that sporadic late onset AD and familial and early onset forms might share a common genetic architecture and that in early onset cohorts the PRS is associated with CSF *p*-tau/Aβ ratio [35]. A PRS has been associated with longitudinal hippocampal thinning in older adults [19], with CSF $A\beta_{42}$ levels [20], and with plasma inflammatory biomarkers [21]. It has been demonstrated that PRS is associated with younger age of AD onset, worse cognitive performance over time, and worse biomarker profile [23] and, recently, with longitudinal cognitive decline in preclinical AD and MCI [26]. However, some authors, when considering a PRS based on nine AD-related risk loci, were not able to show a predictive role in progression from MCI to AD in four independent large cohorts [9]. Our study does not only explore the relationship between PRS and AD biomarkers but, by grouping the 20 risk loci according to their biological role, provides further evidence on the pathways underlying biomarkers changes in the AD continuum (Fig. 3).

Our immune GWS-PRS takes into account the cumulative genetic risk given by the known SNP in the following genes implicated in immune function: *CR1, INPP5D, MEF2C, HLA-DRB5/HLA-DRB1, EPHA1, CLU, MS4A6A, ABCA7,* and *CD33* [36–41]. In our dataset, higher immune GWS-PRS was associated with worse cognitive profile and brain hypometabolism in the angular gyrus, as well as with longitudinal cortical amyloid accumulation. Moreover, it was a significant predictor of brain hypometabolism. Overall, while our data confirm the literature evidence of a strong relationship between brain immune function and Aβ accumulation, they also indicate an association with biomarkers of neurodegeneration and with cognitive status. In particular, while the association between mediators of neuroinflammation and Aβ accumulation and aggregation in early AD stages is well established [42], recent preclinical evidence suggest that the same mediators are also associated with markers of neurodegeneration and with cognitive decline [43–45].

The lipid GWS-PRS score in our study considers the risk alleles of the following genes: *CLU, SORL1*, and *ABCA7* [46]. Our subjects with high lipid GWS-PRS showed increased cortical Aβ levels at baseline and longitudinal brain hypometabolism, indicating that the influence of the three genetic risk variants included in our score is mainly exerted onto Aβ accumulation and brain metabolism. However, we would also have to consider the higher prevalence of *APOE4* carriers in the 90th percentile group of the lipid score. Moreover, probably because only three variants were included in the lipid GWS-PRS, its predictive value over longitudinal biomarker changes was not significant.

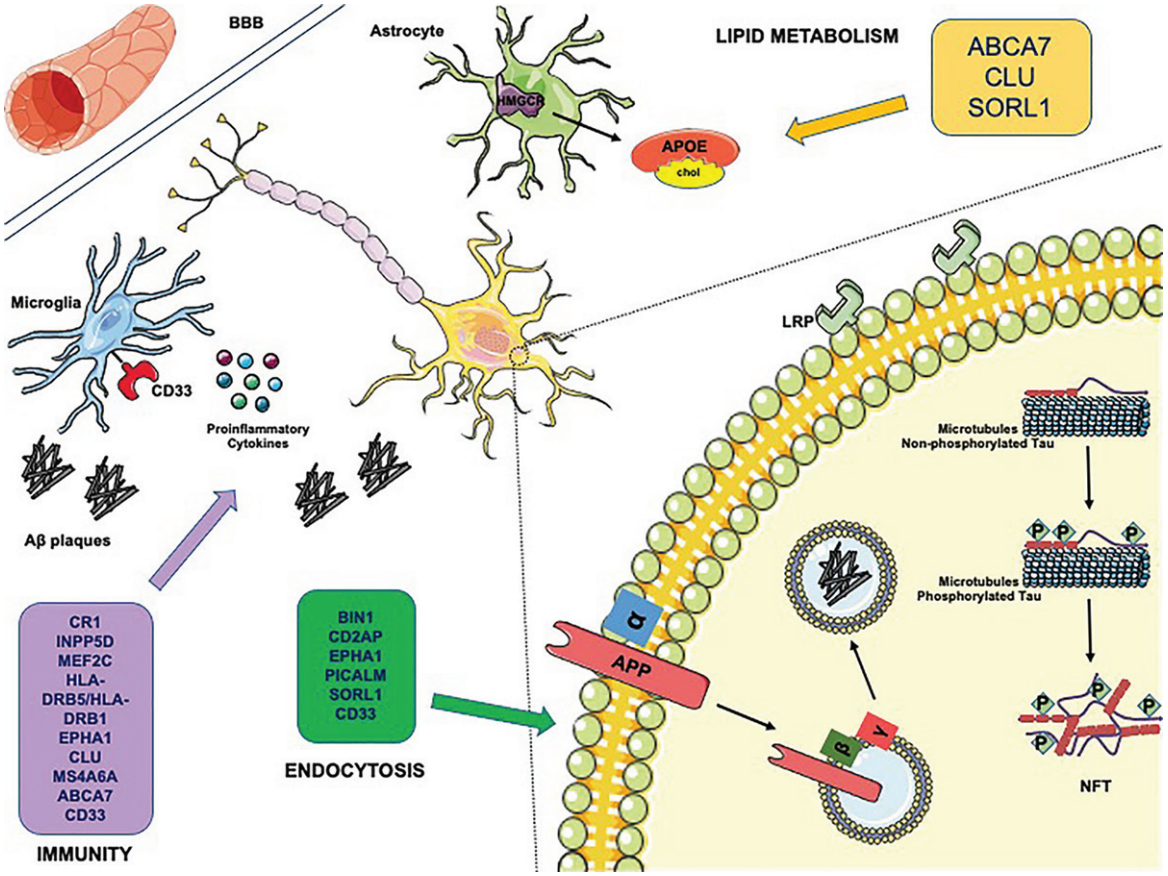

Fig. 3. Genes involved in the immune, lipid, and endocytotic pathways. Schematic representation of how the 20 genes grouped into the polygenic risk scores of immunity, lipid metabolism, and endocytosis might affect the amyloid cascade, neurofibrillary tangles (NFT) formation and neuroinflammation in AD (see text for details on genes function).

The endocytotic GWS-PRS is made of cumulative risk from gene variants in: *BIN1, CD2AP, EPHA1, PICALM, SORL1*, and *CD33* [32, 47, 48]. Probably due to the cumulative effect of the different genes on tau pathology, our endocytotic GWS-PRS showed a significant direct correlation with baseline CSF tau levels in this cohort, despite the small number of subjects for whom CSF data was available.

Some of the known risk variants have not been included in the pathway-specific GWS-PRS but are part of the total GWS-PRS we used in our study. These include: *NME8, ZCWPW1, PTK2B, CELF1, FERMT2, SLC24A4,* and *CASS4* [36, 38, 49–52]. The total GWS-PRS, considering all the genes variants, provides with information related to the cumulative effects of the 20 genes. In our cohort, higher total GWS-PRS was associated with worse cognitive measures, increased [^{18}F]Florbetapir uptake and higher CSF tau levels, as well as with longitudinal cognitive decline and brain hypometabolism. All the aspects of AD pathology are associated with total GWS-PRS, as expected, as this score carries risk from all genes, involved in multiple pathways and overlapping functions.

Although a total GWS-PRS can help stratifying patients according to their cumulative genetic risk, our data suggest that for enrichment strategies in clinical trials the use of specific GWS-PRS looking at the different pathways (immunity, lipid metabolism, endocytosis) might be more effective in selecting the appropriate populations for specific treatment and thus reducing the number of subjects needed to test a specific outcome. Although the associations identified between our GWS-PRS and biomarkers were small, accounting for 1.9%–3.3% of the variance within the population, these effect sizes are consistent with other biomarker studies assessing polygenic

scores [53]. With an approach widely used by other researchers in different fields [54, 55], we stratified our cohort in percentiles of GWS-PRS and compared the bottom (10th percentile) and top (90th percentile) ends of the distribution of GWS-PRS in order to evaluate the differences between subjects in low or high risk categories. Because PRS provide a measure of relative risk for a condition, the percentile value for the individual subject might be more meaningful [56]. Indeed, studies utilizing PRS for targeting specific treatments have shown that for highly prevalent conditions, precision can be better than one in two for the top decile, and most patients will benefit from treatment, so that over half of preventable events can be avoided by targeting just the high-risk decile [57].

While some of the strengths of using the ADNI database are the large sample size, the standardized methodology and detailed biomarkers information, one of the limitations of the present study is that not all measures were available for all biomarkers at the time of data access. In particular, while cognitive data were available on the whole cohort, imaging data were available on a varying subset of subjects according to the modality. Moreover, a 2-year follow up might be too short to look at significant changes associated with genetic risk variants. Indeed, based on available data, 9.5% of the subjects progressed at 2 years and there was no difference in baseline GWS-PRS between stable and progressing participants. However, a longer follow up, as reported by Mormino et al. and others, might have outlined significant longitudinal associations between PRSs and clinical conversion [26, 53]. In addition to that, some of the 20 genes have overlapping functions, thus the results of one PRS are not independent from another PRS. Moreover, replicating these results in larger longitudinal cohorts and expanding the PRS calculation to include novel SNPs would allow for a better understanding of the endophenotypes associated with early changes in AD biomarkers in presymptomatic subjects.

In conclusion, this study highlights that polygenic risk scores can be a good indicator of AD-related changes in biomarkers and cognitive function in a population of HC and MCI subjects with varying degrees of AD risk. In particular, specific risk scores based on the function of genes are associated with different endophenotypes that characterize the AD continuum. This study highlights the influence of different pathways (inflammation, endocytosis, and lipid metabolism) on different pathological process in AD. This is the first study highlighting that immune pathway may influence neurodegeneration affecting amyloid independent pathway, while lipid pathway may be influencing AD through amyloid dependent pathway. These findings underline the importance of enrichment strategies for clinical trials evaluating specific biomarkers for specific treatment. This also highlights the importance of evaluating different pathways further to better understand how different therapeutic strategies could be employed in subsets of AD populations. This also implies that for an effective therapeutic strategy in AD, it may be essential to target immunity, endocytosis, and lipid metabolic pathways.

ACKNOWLEDGMENTS

Data collection and sharing for this project was funded by the Alzheimer's Disease Neuroimaging Initiative (ADNI) (National Institutes of Health Grant U01 AG024904) and DOD ADNI (Department of Defense award number W81XWH-12-2-0012). ADNI is funded by the National Institute on Aging, the National Institute of Biomedical Imaging and Bioengineering, and through generous contributions from the following: AbbVie, Alzheimer's Association; Alzheimer's Drug Discovery Foundation; Araclon Biotech; BioClinica, Inc.; Biogen; Bristol-Myers Squibb Company; CereSpir, Inc.; Cogstate; Eisai Inc.; Elan Pharmaceuticals, Inc.; Eli Lilly and Company; EuroImmun; F. Hoffmann-La Roche Ltd and its affiliated company Genentech, Inc.; Fujirebio; GE Healthcare; IXICO Ltd.; Janssen Alzheimer Immunotherapy Research & Development, LLC.; Johnson & Johnson Pharmaceutical Research & Development LLC.; Lumosity; Lundbeck; Merck & Co., Inc.; Meso Scale Diagnostics, LLC.; NeuroRx Research; Neurotrack Technologies; Novartis Pharmaceuticals Corporation; Pfizer Inc.; Piramal Imaging; Servier; Takeda Pharmaceutical Company; and Transition Therapeutics. The Canadian Institutes of Health Research is providing funds to support ADNI clinical sites in Canada. Private sector contributions are facilitated by the Foundation for the National Institutes of Health (https://www.fnih.org). The grantee organization is the Northern California Institute for Research and Education, and the study is coordinated by the Alzheimer's Therapeutic Research Institute at the University of Southern California. ADNI data are disseminated by the Laboratory for Neuro Imaging at the University of Southern California.

The data that support the findings of this study are available from the corresponding author upon reasonable request.

Authors' disclosures available online (https://www.j-alz.com/manuscript-disclosures/20-0578r2).

SUPPLEMENTARY MATERIAL

The supplementary material is available in the electronic version of this article: https://dx.doi.org/10.3233/JAD-200578.

REFERENCES

[1] Mosconi L (2005) Brain glucose metabolism in the early and specific diagnosis of Alzheimer's disease. FDG-PET studies in MCI and AD. *Eur J Nucl Med Mol Imaging* **32**, 486-510.

[2] World Health Organization, Global Dementia Observatory, https://www.who.int/mental_health/neurology/dementia/GDO/en/.

[3] Bettens K, Sleegers K, Van Broeckhoven C (2013) Genetic insights in Alzheimer's disease. *Lancet Neurol* **12**, 92-104.

[4] Scheltens P, Blennow K, Breteler MM, de Strooper B, Frisoni GB, Salloway S, Van der Flier WM (2016) Alzheimer's disease. *Lancet* **388**, 505-517.

[5] Espinosa A, Alegret M, Valero S, Vinyes-Junque G, Hernandez I, Mauleon A, Rosende-Roca M, Ruiz A, Lopez O, Tarraga L, Boada M (2013) A longitudinal follow-up of 550 mild cognitive impairment patients: Evidence for large conversion to dementia rates and detection of major risk factors involved. *J Alzheimers Dis* **34**, 769-780.

[6] Weiner MW, Veitch DP, Aisen PS, Beckett LA, Cairns NJ, Green RC, Harvey D, Jack CR, Jr., Jagust W, Morris JC, Petersen RC, Saykin AJ, Shaw LM, Toga AW, Trojanowski JQ, Alzheimer's Disease Neuroimaging Initiative (2017) Recent publications from the Alzheimer's Disease Neuroimaging Initiative: Reviewing progress toward improved AD clinical trials. *Alzheimers Dement* **13**, e1-e85.

[7] Gainotti G (2010) Origins, controversies and recent developments of the MCI construct. *Curr Alzheimer Res* **7**, 271-279.

[8] Drago V, Babiloni C, Bartres-Faz D, Caroli A, Bosch B, Hensch T, Didic M, Klafki HW, Pievani M, Jovicich J, Venturi L, Spitzer P, Vecchio F, Schoenknecht P, Wiltfang J, Redolfi A, Forloni G, Blin O, Irving E, Davis C, Hardemark HG, Frisoni GB (2011) Disease tracking markers for Alzheimer's disease at the prodromal (MCI) stage. *J Alzheimers Dis* **26 Suppl 3**, 159-199.

[9] Lacour A, Espinosa A, Louwersheimer E, Heilmann S, Hernandez I, Wolfsgruber S, Fernandez V, Wagner H, Rosende-Roca M, Mauleon A, Moreno-Grau S, Vargas L, Pijnenburg YA, Koene T, Rodriguez-Gomez O, Ortega G, Ruiz S, Holstege H, Sotolongo-Grau O, Kornhuber J, Peters O, Frolich L, Hull M, Ruther E, Wiltfang J, Scherer M, Riedel-Heller S, Alegret M, Nothen MM, Scheltens P, Wagner M, Tarraga L, Jessen F, Boada M, Maier W, van der Flier WM, Becker T, Ramirez A, Ruiz A (2017) Genome-wide significant risk factors for Alzheimer's disease: Role in progression to dementia due to Alzheimer's disease among subjects with mild cognitive impairment. *Mol Psychiatry* **22**, 153-160.

[10] Barber IS, Braae A, Clement N, Patel T, Guetta-Baranes T, Brookes K, Medway C, Chappell S, Guerreiro R, Bras J, Hernandez D, Singleton A, Hardy J, Mann DM, Consortium A, Morgan K (2017) Mutation analysis of sporadic early-onset Alzheimer's disease using the NeuroX array. *Neurobiol Aging* **49**, 215.e1-215.e8.

[11] Karch CM, Cruchaga C, Goate AM (2014) Alzheimer's disease genetics: From the bench to the clinic. *Neuron* **83**, 11-26.

[12] Harold D, Abraham R, Hollingworth P, Sims R, Gerrish A, Hamshere ML, Pahwa JS, Moskvina V, Dowzell K, Williams A, Jones N, Thomas C, Stretton A, Morgan AR, Lovestone S, Powell J, Proitsi P, Lupton MK, Brayne C, Rubinsztein DC, Gill M, Lawlor B, Lynch A, Morgan K, Brown KS, Passmore PA, Craig D, McGuinness B, Todd S, Holmes C, Mann D, Smith AD, Love S, Kehoe PG, Hardy J, Mead S, Fox N, Rossor M, Collinge J, Maier W, Jessen F, Schurmann B, Heun R, van den Bussche H, Heuser I, Kornhuber J, Wiltfang J, Dichgans M, Frolich L, Hampel H, Hull M, Rujescu D, Goate AM, Kauwe JS, Cruchaga C, Nowotny P, Morris JC, Mayo K, Sleegers K, Bettens K, Engelborghs S, De Deyn PP, Van Broeckhoven C, Livingston G, Bass NJ, Gurling H, McQuillin A, Gwilliam R, Deloukas P, Al-Chalabi A, Shaw CE, Tsolaki M, Singleton AB, Guerreiro R, Muhleisen TW, Nothen MM, Moebus S, Jockel KH, Klopp N, Wichmann HE, Carrasquillo MM, Pankratz VS, Younkin SG, Holmans PA, O'Donovan M, Owen MJ, Williams J (2009) Genome-wide association study identifies variants at CLU and PICALM associated with Alzheimer's disease. *Nat Genet* **41**, 1088-1093.

[13] Lambert JC, Ibrahim-Verbaas CA, Harold D, Naj AC, Sims R, Bellenguez C, DeStafano AL, Bis JC, Beecham GW, Grenier-Boley B, et al. (2013) Meta-analysis of 74,046 individuals identifies 11 new susceptibility loci for Alzheimer's disease. *Nat Genet* **45**, 1452-1458.

[14] Tosto G, Reitz C (2013) Genome-wide association studies in Alzheimer's disease: A review. *Curr Neurol Neurosci Rep* **13**, 381.

[15] Seshadri S, Fitzpatrick AL, Ikram MA, DeStefano AL, Gudnason V, Boada M, Bis JC, Smith AV, Carassquillo MM, Lambert JC, Harold D, Schrijvers EM, Ramirez-Lorca R, Debette S, Longstreth WT, Jr., Janssens AC, Pankratz VS, Dartigues JF, Hollingworth P, Aspelund T, Hernandez I, Beiser A, Kuller LH, Koudstaal PJ, Dickson DW, Tzourio C, Abraham R, Antunez C, Du Y, Rotter JI, Aulchenko YS, Harris TB, Petersen RC, Berr C, Owen MJ, Lopez-Arrieta J, Varadarajan BN, Becker JT, Rivadeneira F, Nalls MA, Graff-Radford NR, Campion D, Auerbach S, Rice K, Hofman A, Jonsson PV, Schmidt H, Lathrop M, Mosley TH, Au R, Psaty BM, Uitterlinden AG, Farrer LA, Lumley T, Ruiz A, Williams J, Amouyel P, Younkin SG, Wolf PA, Launer LJ, Lopez OL, van Duijn CM, Breteler MM, CHARGE Consortium; GERAD1 Consortium; EADI1 Consortium (2010) Genome-wide analysis of genetic loci associated with Alzheimer disease. *JAMA* **303**, 1832-1840.

[16] Naj AC, Jun G, Beecham GW, Wang LS, Vardarajan BN, Buros J, Gallins PJ, Buxbaum JD, Jarvik GP, Crane PK, et al. (2011) Common variants at MS4A4/MS4A6E, CD2AP, CD33 and EPHA1 are associated with late-onset Alzheimer's disease. *Nat Genet* **43**, 436-441.

[17] Kunkle BW, Grenier-Boley B, Sims R, Bis JC, Damotte V, Naj AC, Boland A, Vronskaya M, van der Lee SJ, Amlie-Wolf A, et al. (2019) Author Correction: Genetic

meta-analysis of diagnosed Alzheimer's disease identifies new risk loci and implicates Abeta, tau, immunity and lipid processing. *Nat Genet* **51**, 1423-1424.

[18] Jansen IE, Savage JE, Watanabe K, Bryois J, Williams DM, Steinberg S, Sealock J, Karlsson IK, Hagg S, Athanasiu L, Voyle N, Proitsi P, Witoelar A, Stringer S, Aarsland D, Almdahl IS, Andersen F, Bergh S, Bettella F, Bjornsson S, Braekhus A, Brathen G, de Leeuw C, Desikan RS, Djurovic S, Dumitrescu L, Fladby T, Hohman TJ, Jonsson PV, Kiddle SJ, Rongve A, Saltvedt I, Sando SB, Selbaek G, Shoai M, Skene NG, Snaedal J, Stordal E, Ulstein ID, Wang Y, White LR, Hardy J, Hjerling-Leffler J, Sullivan PF, van der Flier WM, Dobson R, Davis LK, Stefansson H, Stefansson K, Pedersen NL, Ripke S, Andreassen OA, Posthuma D (2019) Genome-wide meta-analysis identifies new loci and functional pathways influencing Alzheimer's disease risk. *Nat Genet* **51**, 404-413.

[19] Harrison TM, Mahmood Z, Lau EP, Karacozoff AM, Burggren AC, Small GW, Bookheimer SY (2016) An Alzheimer's disease genetic risk score predicts longitudinal thinning of hippocampal complex subregions in healthy older adults. *eNeuro* **3**, ENEURO.0098-16.2016.

[20] Martiskainen H, Helisalmi S, Viswanathan J, Kurki M, Hall A, Herukka SK, Sarajarvi T, Natunen T, Kurkinen KM, Huovinen J, Makinen P, Laitinen M, Koivisto AM, Mattila KM, Lehtimaki T, Remes AM, Leinonen V, Haapasalo A, Soininen H, Hiltunen M (2015) Effects of Alzheimer's disease-associated risk loci on cerebrospinal fluid biomarkers and disease progression: A polygenic risk score approach. *J Alzheimers Dis* **43**, 565-573.

[21] Morgan AR, Touchard S, O'Hagan C, Sims R, Majounie E, Escott-Price V, Jones L, Williams J, Morgan BP (2017) The correlation between inflammatory biomarkers and polygenic risk score in Alzheimer's disease. *J Alzheimers Dis* **56**, 25-36.

[22] Chaudhury S, Patel T, Barber IS, Guetta-Baranes T, Brookes KJ, Chappell S, Turton J, Guerreiro R, Bras J, Hernandez D, Singleton A, Hardy J, Mann D, ARUK Consortium, Morgan K (2018) Polygenic risk score in postmortem diagnosed sporadic early-onset Alzheimer's disease. *Neurobiol Aging* **62**, 244 e241-244 e248.

[23] Desikan RS, Fan CC, Wang Y, Schork AJ, Cabral HJ, Cupples LA, Thompson WK, Besser L, Kukull WA, Holland D, Chen CH, Brewer JB, Karow DS, Kauppi K, Witoelar A, Karch CM, Bonham LW, Yokoyama JS, Rosen HJ, Miller BL, Dillon WP, Wilson DM, Hess CP, Pericak-Vance M, Haines JL, Farrer LA, Mayeux R, Hardy J, Goate AM, Hyman BT, Schellenberg GD, McEvoy LK, Andreassen OA, Dale AM (2017) Genetic assessment of age-associated Alzheimer disease risk: Development and validation of a polygenic hazard score. *PLoS Med* **14**, e1002258.

[24] Escott-Price V, Sims R, Bannister C, Harold D, Vronskaya M, Majounie E, Badarinarayan N; GERAD/PERADES; IGAP consortia; Morgan K, Passmore P, Holmes C, Powell J, Brayne C, Gill M, Mead S, Goate A, Cruchaga C, Lambert JC, van Duijn C, Maier W, Ramirez A, Holmans P, Jones L, Hardy J, Seshadri S, Schellenberg GD, Amouyel P, Williams J (2015) Common polygenic variation enhances risk prediction for Alzheimer's disease. *Brain* **138**, 3673-3684.

[25] Chouraki V, Reitz C, Maury F, Bis JC, Bellenguez C, Yu L, Jakobsdottir J, Mukherjee S, Adams HH, Choi SH, Larson EB, Fitzpatrick A, Uitterlinden AG, de Jager PL, Hofman A, Gudnason V, Vardarajan B, Ibrahim-Verbaas C, van der Lee SJ, Lopez O, Dartigues JF, Berr C, Amouyel P, Bennett DA, van Duijn C, DeStefano AL, Launer LJ, Ikram MA, Crane PK, Lambert JC, Mayeux R, Seshadri S, International Genomics of Alzheimer's Project (2016) Evaluation of a genetic risk score to improve risk prediction for Alzheimer's disease. *J Alzheimers Dis* **53**, 921-932.

[26] Tan CH, Hyman BT, Tan JJX, Hess CP, Dillon WP, Schellenberg GD, Besser LM, Kukull WA, Kauppi K, McEvoy LK, Andreassen OA, Dale AM, Fan CC, Desikan RS (2017) Polygenic hazard scores in preclinical Alzheimer disease. *Ann Neurol* **82**, 484-488.

[27] Caspers S, Rockner ME, Jockwitz C, Bittner N, Teumer A, Herms S, Hoffmann P, Nothen MM, Moebus S, Amunts K, Cichon S, Muhleisen TW (2020) Pathway-specific genetic risk for Alzheimer's disease differentiates regional patterns of cortical atrophy in older adults. *Cereb Cortex* **30**, 801-811.

[28] Darst BF, Koscik RL, Racine AM, Oh JM, Krause RA, Carlsson CM, Zetterberg H, Blennow K, Christian BT, Bendlin BB, Okonkwo OC, Hogan KJ, Hermann BP, Sager MA, Asthana S, Johnson SC, Engelman CD (2017) Pathway-specific polygenic risk scores as predictors of amyloid-beta deposition and cognitive function in a sample at increased risk for Alzheimer's disease. *J Alzheimers Dis* **55**, 473-484.

[29] Sabuncu MR, Buckner RL, Smoller JW, Lee PH, Fischl B, Sperling RA, Alzheimer's Disease Neuroimaging Initiative (2012) The association between a polygenic Alzheimer score and cortical thickness in clinically normal subjects. *Cereb Cortex* **22**, 2653-2661.

[30] Landau S, Jagust W (2011) UC Berkeley FDG MetaROI methods. Alzheimer's Disease Neuroimaging Initiative.

[31] Landau S, Jagust W. (2015) Florbetapir processing methods. Alzheimer's Disease Neuroimaging Initiative.

[32] Chouraki V, Seshadri S (2014) Genetics of Alzheimer's disease. *Adv Genet* **87**, 245-294.

[33] Escott-Price V, Myers AJ, Huentelman M, Hardy J (2017) Polygenic risk score analysis of pathologically confirmed Alzheimer disease. *Ann Neurol* **82**, 311-314.

[34] Marden JR, Mayeda ER, Walter S, Vivot A, Tchetgen Tchetgen EJ, Kawachi I, Glymour MM (2016) Using an Alzheimer disease polygenic risk score to predict memory decline in black and white Americans over 14 years of follow-up. *Alzheimer Dis Assoc Disord* **30**, 195-202.

[35] Cruchaga C, Del-Aguila JL, Saef B, Black K, Fernandez MV, Budde J, Ibanez L, Deming Y, Kapoor M, Tosto G, Mayeux RP, Holtzman DM, Fagan AM, Morris JC, Bateman RJ, Goate AM, Dominantly Inherited Alzheimer Network (DIAN); Disease Neuroimaging Initiative (ADNI); NIA-LOAD family study; Harari O (2018) Polygenic risk score of sporadic late-onset Alzheimer's disease reveals a shared architecture with the familial and early-onset forms. *Alzheimers Dement* **14**, 205-214.

[36] Karch CM, Goate AM (2015) Alzheimer's disease risk genes and mechanisms of disease pathogenesis. *Biol Psychiatry* **77**, 43-51.

[37] Zhu XC, Yu JT, Jiang T, Wang P, Cao L, Tan L (2015) CR1 in Alzheimer's disease. *Mol Neurobiol* **51**, 753-765.

[38] Stage E, Duran T, Risacher SL, Goukasian N, Do TM, West JD, Wilhalme H, Nho K, Phillips M, Elashoff D, Saykin AJ, Apostolova LG (2016) The effect of the top 20 Alzheimer disease risk genes on gray-matter density and FDG PET brain metabolism. *Alzheimers Dement (Amst)* **5**, 53-66.

[39] Wang HF, Tan L, Hao XK, Jiang T, Tan MS, Liu Y, Zhang DQ, Yu JT, Alzheimer's Disease Neuroimaging Initiative (2015) Effect of EPHA1 genetic variation on cere-

brospinal fluid and neuroimaging biomarkers in healthy, mild cognitive impairment and Alzheimer's disease cohorts. *J Alzheimers Dis* **44**, 115-123.

[40] Li H, Karl T, Garner B (2015) Understanding the function of ABCA7 in Alzheimer's disease. *Biochem Soc Trans* **43**, 920-923.

[41] Jiang T, Yu JT, Hu N, Tan MS, Zhu XC, Tan L (2014) CD33 in Alzheimer's disease. *Mol Neurobiol* **49**, 529-535.

[42] Heppner FL, Ransohoff RM, Becher B (2015) Immune attack: The role of inflammation in Alzheimer disease. *Nat Rev Neurosci* **16**, 358-372.

[43] Domingues C, da Cruz ESOAB, Henriques AG (2017) Impact of cytokines and chemokines on Alzheimer's Disease neuropathological hallmarks. *Curr Alzheimer Res* **14**, 870-882.

[44] Griciuc A, Patel S, Federico AN, Choi SH, Innes BJ, Oram MK, Cereghetti G, McGinty D, Anselmo A, Sadreyev RI, Hickman SE, El Khoury J, Colonna M, Tanzi RE (2019) TREM2 acts downstream of CD33 in modulating microglial pathology in Alzheimer's disease. *Neuron* **103**, 820-835 e827.

[45] Carlock C, Wu J, Shim J, Moreno-Gonzalez I, Pitcher MR, Hicks J, Suzuki A, Iwata J, Quevado J, Lou Y (2017) Interleukin33 deficiency causes tau abnormality and neurodegeneration with Alzheimer-like symptoms in aged mice. *Transl Psychiatry* **7**, e1164.

[46] Andersen OM, Rudolph IM, Willnow TE (2016) Risk factor SORL1: From genetic association to functional validation in Alzheimer's disease. *Acta Neuropathol* **132**, 653-665.

[47] Tan MS, Yu JT, Tan L (2013) Bridging integrator 1 (BIN1): Form, function, and Alzheimer's disease. *Trends Mol Med* **19**, 594-603.

[48] Xu W, Tan L, Yu JT (2015) The role of PICALM in Alzheimer's disease. *Mol Neurobiol* **52**, 399-413.

[49] Liu Y, Yu JT, Wang HF, Hao XK, Yang YF, Jiang T, Zhu XC, Cao L, Zhang DQ, Tan L (2014) Association between NME8 locus polymorphism and cognitive decline, cerebrospinal fluid and neuroimaging biomarkers in Alzheimer's disease. *PLoS One* **9**, e114777.

[50] Dourlen P, Fernandez-Gomez FJ, Dupont C, Grenier-Boley B, Bellenguez C, Obriot H, Caillierez R, Sottejeau Y, Chapuis J, Bretteville A, Abdelfettah F, Delay C, Malmanche N, Soininen H, Hiltunen M, Galas MC, Amouyel P, Sergeant N, Buee L, Lambert JC, Dermaut B (2017) Functional screening of Alzheimer risk loci identifies PTK2B as an *in vivo* modulator and early marker of Tau pathology. *Mol Psychiatry* **22**, 874-883.

[51] Chapuis J, Flaig A, Grenier-Boley B, Eysert F, Pottiez V, Deloison G, Vandeputte A, Ayral AM, Mendes T, Desai S, Goate AM, Kauwe JSK, Leroux F, Herledan A, Demiautte F, Bauer C, Checler F, Petersen RC, Blennow K, Zetterberg H, Minthon L, Van Deerlin VM, Lee VM, Shaw LM, Trojanowski JQ, Albert M, Moghekar A, O'Brien R, Peskind ER, Malmanche N, Schellenberg GD, Dourlen P, Song OR, Cruchaga C, Amouyel P, Deprez B, Brodin P, Lambert JC, ADGC, Alzheimer's Disease Neuroimaging Initiative (2017) Genome-wide, high-content siRNA screening identifies the Alzheimer's genetic risk factor FERMT2 as a major modulator of APP metabolism. *Acta Neuropathol* **133**, 955-966.

[52] Hinney A, Albayrak O, Antel J, Volckmar AL, Sims R, Chapman J, Harold D, Gerrish A, Heid IM, Winkler TW, Scherag A, Wiltfang J, Williams J, Hebebrand J, GERAD Consortium; IGAP Consortium; GIANT Consortium (2014) Genetic variation at the CELF1 (CUGBP, elav-like family member 1 gene) locus is genome-wide associated with Alzheimer's disease and obesity. *Am J Med Genet B Neuropsychiatr Genet* **165B**, 283-293.

[53] Mormino EC, Sperling RA, Holmes AJ, Buckner RL, De Jager PL, Smoller JW, Sabuncu MR, Alzheimer's Disease Neuroimaging Initiative (2016) Polygenic risk of Alzheimer disease is associated with early- and late-life processes. *Neurology* **87**, 481-488.

[54] Thompson MD, Pirkle CM, Youkhana F, Wu YY (2020) Gene-obesogenic environment interactions on body mass indices for older black and white men and women from the Health and Retirement Study. *Int J Obes (Lond)* **44**, 1893-1905.

[55] Lall K, Lepamets M, Palover M, Esko T, Metspalu A, Tonisson N, Padrik P, Magi R, Fischer K (2019) Polygenic prediction of breast cancer: Comparison of genetic predictors and implications for risk stratification. *BMC Cancer* **19**, 557.

[56] Lewis CM, Vassos E (2020) Polygenic risk scores: From research tools to clinical instruments. *Genome Med* **12**, 44.

[57] Gibson G (2019) On the utilization of polygenic risk scores for therapeutic targeting. *PLoS Genet* **15**, e1008060.